VEHICLE SYSTEM DYNAMICS
https://doi.org/10.1080/00423114.2025.2556928

OPEN ACCESS Check for updates

A 4WD drift assist control framework on general rally track

Yiwen Sun[a], Efstathios Velenis[a] and Ajinkya Krishnakumar[b]

[a]Advanced Vehicle Engineering Centre, Cranfield University, Bedford, UK; [b]Rimac Technology, Zagreb, Croatia

ABSTRACT

In this paper, we present a novel state machine-based 4-Wheel-Drive (4WD) drift assist controller with four drive modes, to allow the driver transition into and out of drifting in corners intuitively. To interpret the driver's intention to drift, we rely on the driver's inputs and vehicle motion signals. During drifting, without prior knowledge of path geometry, we introduce a 'Trajectory Radius Predictor' to assist the driver stay on the desired course and provide the necessary reference yaw rate for the subsequent torque vectoring controller. Additionally, we restrict the sideslip rate to allow the driver sufficient reaction time to counter steer and follow the desired track when the sideslip changes during drifting. To validate our controller, we consider different driving behaviours from both the CarMaker driver model and a human driver using the driving simulator of Cranfield University. The Pikes Peak rally track in IPG CarMaker is utilised for evaluation, and the results have demonstrated the effectiveness of the proposed framework.

ARTICLE HISTORY
Received 8 July 2024
Revised 27 August 2025
Accepted 29 August 2025

KEYWORDS
Drift assist control; torque vectoring; vehicle dynamics and control

Introduction

Drifting, a unique cornering technique characterised by high sideslip and counter steering (yaw rate direction opposite to the steering input) [1], generally requires advanced driving skills from professional drivers or the intervention of a sophisticated control system. The rear axle is first saturated by handbrake [2–4], throttle [5] or pendulum-turn [6,7] to enter drifting, and then a subtle coordination of throttle and steering is crucial to maintain an unstable power sliding equilibrium of the vehicle dynamics [8,9].

Extensive attention has been given to autonomous drifting in previous research, where it is essential to have prior knowledge of the path geometry. Using knowledge of the desired trajectory radius from either a circular track [10–14] or the path-following controller in a complex shape track [15–18], drift equilibria can be calculated with a single-track [19–21] or double-track vehicle model [11], and utilised as target states for the subsequent control using various methods (proportional feedback [13,22,23], LQR [11,24], MPC [25–30]). However, when it comes to drift assist control in the context of Advanced Driver Assist System (ADAS), where the driver is responsible for path tracking, the lack of knowledge of the desired path poses a challenge for the following drift equilibrium calculation and motion control.

CONTACT Efstathios Velenis e.velenis@cranfield.ac.uk

© 2025 The Author(s). Published by Informa UK Limited, trading as Taylor & Francis Group.
This is an Open Access article distributed under the terms of the Creative Commons Attribution License (http://creativecommons.org/licenses/by/4.0/), which permits unrestricted use, distribution, and reproduction in any medium, provided the original work is properly cited. The terms on which this article has been published allow the posting of the Accepted Manuscript in a repository by the author(s) or with their consent.

For the transition from normal cornering to drifting, the handling dynamics phase portrait [19] indicates that drifting could only be initiated when the vehicle is in an unstable region, which could be easily reached by open-loop control [31] by applying full throttle and maximum steering until both the yaw rate and the sideslip exceed a certain threshold. Besides these thresholds, [32] introduces a button on the dashboard to activate/deactivate the drift mode with a fixed target slip ratio, [33] considers the product of steering and yaw rate to identify driver's counter steering behaviour, while [34] utilises full throttle as a trigger to increase sideslip until counter steering is detected. Nevertheless, the above methods can only cover limited scenarios (circular track [32,34] or U-turn [33]), and few studies have considered complex road formations, such as rally tracks, or designed a system that allows human drivers to enter/exit drifting intuitively in the desired corner.

For the present drift assist control deployed on high-performance rear-wheel-drive (RWD) vehicles (i.e. BMW [35], McLaren [36]) utilising active differentials, more torque could be distributed to either side of the rear axle for power sliding [37]. However, although theoretically the throttle and steering could be used to stabilise the sideslip and yaw rate respectively [14,32,38,39], professional driving skills especially proper steering reaction from the human driver are still required [35] to control the lateral force of the front axle, which has to be subtly coordinated with throttle and sideslip to follow the desired trajectory according to drift equilibria analysis [19].

A 4-wheel-drive (4WD) configuration, which allows independent wheel torque control, not only offers more drift equilibria [40] and possibilities for hierarchical controller structure [41–43], but also results in an over actuated system where the need for precalculated drift equilibrium as target for drift control is eliminated: as shown in [44–46] a simple feedback structure for 4WD drift control can be implemented to regulate the vehicle's yaw rate and sideslip.

Based on the discussion above, in this paper we present an intuitive 4WD drift assist control framework that can detect the driver's intention to drift and allows them to transition from normal driving to drifting in the desired corners along any path without prior knowledge of the path's geometry. The proposed framework uses the advantages provided by 4WD and torque vectoring. The novelty of this work is summarised as follows.

First, to assist the driver drift intuitively along the desired corners without deviating from the track or losing control, a state machine structure with four drive modes is developed to allow the driver transition into and out of drifting in corners smoothly and effortlessly resume normal driving on straight roads.

Second, to comprehend the driver's intention to start/exit drifting at the desired moment, no extra control inputs (i.e. buttons [32]) or sensors are utilised as switches to activate/deactivate drifting in our work. Instead, we rely on driver inputs, and available vehicle motion signals to identify the driver's desire to drift, which we refer to as 'Drift Intention'.

Third, in contrast to previous studies rely on map-based path knowledge [16,47] or track radius [15], we introduce a 'Trajectory Radius Predictor' to predict the path radius according to real-time data, to assist the driver drift on course and provide a reference yaw rate to the subsequent torque vectoring controller.

Additionally, for the low-level drift controller, we utilise the over-actuated nature of 4WD torque vectoring with independent torque control [44–46,48] so a comprehensive equilibrium map is not required as the control reference. Besides, to assist non-expert

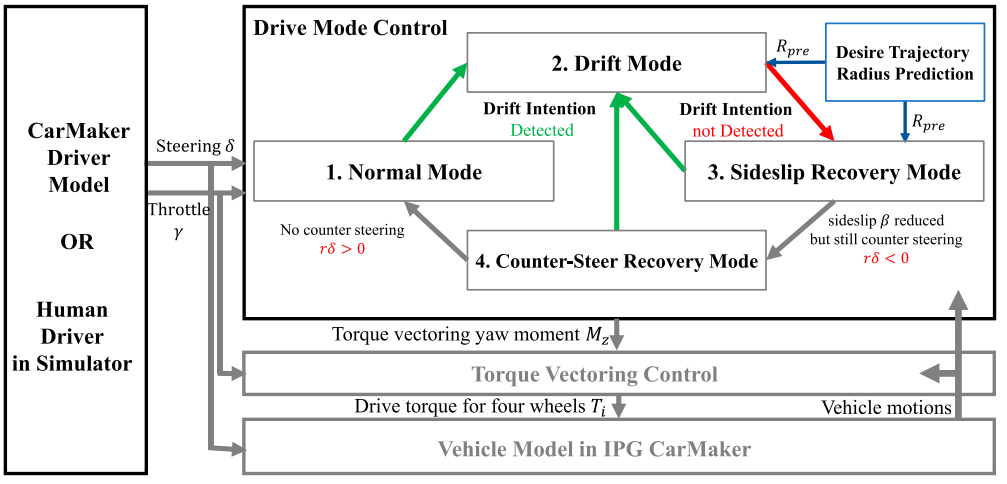


Figure 1. The proposed control framework.

drivers perform drifting, we adopt the idea of interpreting the desired sideslip angle through throttle input, meanwhile restricting the sideslip rate and stabilising the path angle rate, which is proposed in our previous work [49] and evaluated through a human trial. This paper further validates this design on a complex shape rally track in the driving simulator of Cranfield University.

The drift assist control framework

State machine-based drift assist control with four drive modes

As shown in Figures 1 and 2, the state machine structure for the proposed drift assist control includes four modes: Normal Mode, Drift Mode, Sideslip Recovery Mode and Counter-Steer Recovery Mode.

In Normal Mode (Mode 1), the vehicle performs normal cornering and the torque vectoring controller contributes to neutral steering. Subsequently, after detecting the driver's Drift Intention while entering the corners, the vehicle transits to Drift Mode (Mode 2), in which high sideslip will be generated by torque vectoring (TVC in Figure 2). Meanwhile, the future trajectory radius will be predicted by the Trajectory Radius Predictor and the sideslip rate will be constrained to allow the driver enough reaction time to perform counter steering and drift along the desired corner intuitively. Once the Drift Intention is no longer detected while the vehicle exits the corner, the system switches to Sideslip Recovery Mode (Mode 3), where the target sideslip for the torque vectoring controller is set to zero, and the driver is expected to steer towards neutral position from counter steering while the sideslip is decreasing. In addition, when the sideslip is reduced but counter steering is still present (i.e. when driver doesn't steer back from counter steering timely enough), the vehicle will enter Counter-Steer Recovery Mode (Mode 4), during which the trajectory radius is not taken into consideration, and the focus is solely on stabilising the sideslip until there is no more counter steering, then the vehicle switches back to Normal Mode (Mode 1). Details about these drive modes will be provided in the following sections.

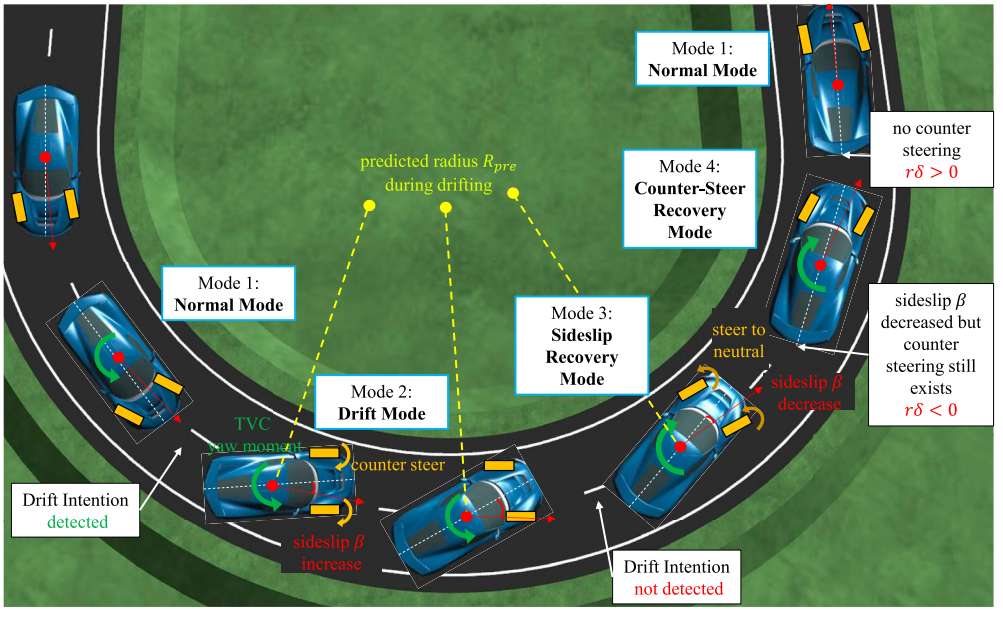


Figure 2. The transition between four drive modes in a corner.

The Normal Mode (Mode 1)

Since drifting can be described as cornering with high yaw rate (oversteer) to achieve high sideslip, for a consistent handling feel, in Normal Mode (Mode 1 in Figure 1) the vehicle is set to neutral steer rather than understeer for a smoother transition from Normal Mode to Drift Mode (Mode 2).

Considering a single-track vehicle model and neglecting tire sideslip, the ideal yaw rate r_d is denoted as (1), in which v_x is the longitudinal velocity, δ is the steering angle of the front wheel, and L is the wheelbase of the vehicle.

$$r_d = v_x \tan \delta / L \tag{1}$$

With the error between the ideal yaw rate r_d and the actual yaw rate r, a proportional–integral (PI) controller is implemented to calculate the additional yaw moment M_z demanded from the subsequent section of torque vectoring controller, as shown in (2) and (3), in which k_p and k_i are coefficients calibrated though driver-in-loop tests.

$$e_r = r_d - r \tag{2}$$

$$M_z = k_p e_r + k_i \int e_r dt \tag{3}$$

The detection of the driver's drift intention

To transition from normal cornering to drifting (Mode 1 to Mode 2 in Figure 1) at the desired moment, we don't rely on preplanned manoeuvres [15,16] or use of additional control inputs (i.e. button [32,39]) from the driver. Instead, we only rely on pedals, steering wheel and other vehicle motion signals to detect the driver's desire to drift, which we refer to as 'Drift Intention'.

The initial step to perform drifting for the driver is to approach the speed limit according to the road friction in the given corner, this is crucial as drifting requires the rear tires to be fully saturated while the front tires being nearly fully saturated [5,20], and the longitudinal acceleration contributes more in the centripetal direction. In this context, we assume the speed limit v_{lim} could be simply written as (4), in which μ is the tire/road adhesion coefficient (an adhesion coefficient estimator will be introduced in our future work), and R_{pre} is the predicted trajectory radius in the corner due to the absence of prior knowledge about path geometry, a topic that will be further elaborated in the next section of Trajectory Radius Predictor.

$$v_{lim} = \sqrt{\mu g R_{pre}} \tag{4}$$

To detect the driver's Drift Intention, we not only compare the current vehicle speed v with the speed limit v_{lim} but also consider the driver's acceleration demand a_d and the predicted speed in the future timesteps v_d, which could be written as (5) and (6) respectively, in which the total longitudinal drive force F_{xcmd} is a function of throttle value γ and the current speed v, m is the vehicle mass, and Δt is the timestep size ($\Delta t = 0.5$ s).

$$a_d = F_{xcmd}/m = f(\gamma, v)/m \tag{5}$$

$$v_d = v + a_d \Delta t \tag{6}$$

With the above discussion, the criteria to detect Drift Intention could be summarised in (7), where $k_v = 0.85, k_{vd} = 0.9$ are the derating factors for the speeds of v, v_d respectively, to tolerate the error in the calculation of v_{lim}(4), and most importantly to activate the Drift Mode with sideslip control before the vehicle reaches the actual friction limit and loses control (spins due to the torque vectoring that saturates the rear axle before the front) in Normal Mode. In detail, the conditions of v and v_d are designed to consider two specific throttle behaviours before drifting: the first is to accelerate smoothly to $v > k_v v_{lim}$; the second is to apply full throttle and produce an abrupt torque request to satisfy the condition of $v_d > k_{vd} v_{lim}$. In fact, the second behaviour is similar to real-world power sliding [5,8,32] where an abrupt torque is produced to saturate the rear axle and initiate drifting. However, in this paper the sideslip during drifting is produced and regulated by the torque vectoring in the Drift Mode.

$$(v > k_v v_{lim} || v_d > k_{vd} v_{lim}) \text{ AND } (\gamma > 0) \tag{7}$$

The trajectory radius predictor

In previous studies [15] on drift control, the prior knowledge of trajectory (or path) radius R is essential as a premise for subsequent control design. The path radius is directly linked to the path angle rate $\dot{\varphi}$ as shown in (8), which is a combination of the yaw rate r and the sideslip rate $\dot{\beta}$, therefore plays a critical role in the subsequent sideslip stabilisation and yaw rate control for drift trajectory tracking.

$$\frac{v}{R} = \dot{\varphi} = r + \dot{\beta} \tag{8}$$

In contrast to autonomous drifting with prior path planning, for drift assist control we have to treat the trajectory radius as an unknown variable that requires prediction (the Desired

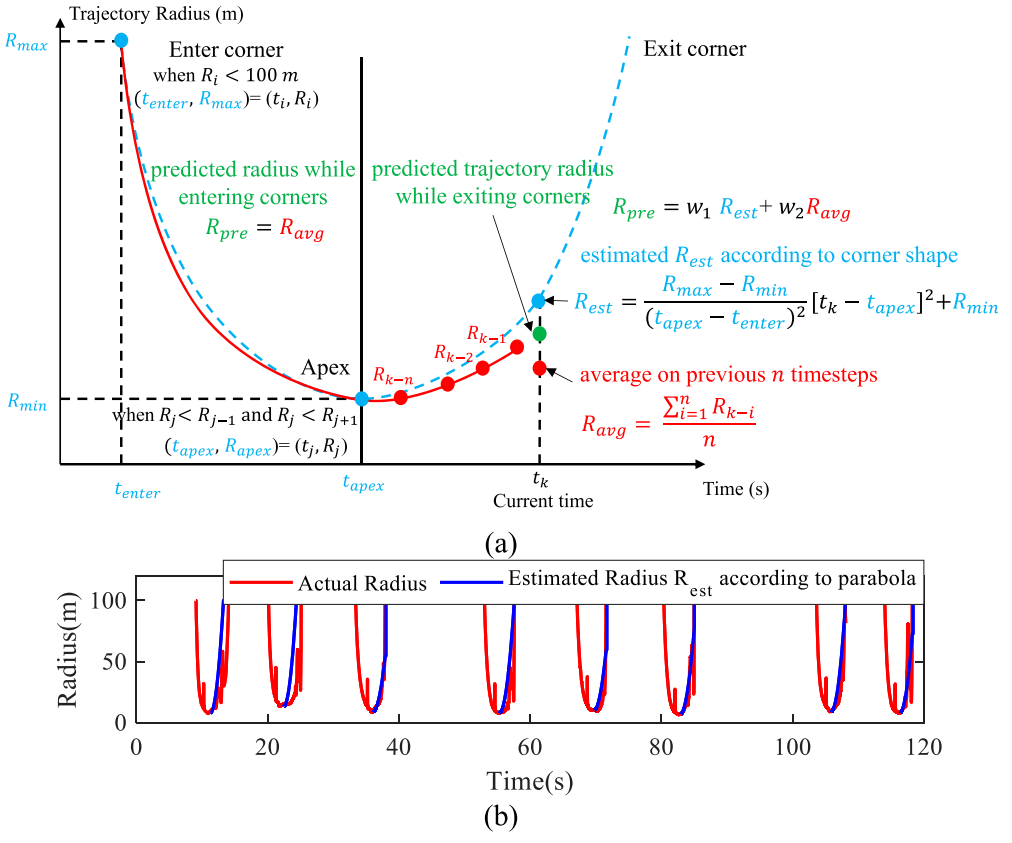


Figure 3. The trajectory radius predictor (a) and the estimated radius R_{est} in the exit of corners on a rally track according to parabola (b).

Trajectory Radius Prediction block in Figure 1). In addition to its association with sideslip and yaw rate control as mentioned in (8), it is also noteworthy that one of the goals in Drift Mode (elaborated in the subsequent section) is to minimise its impact on trajectory radius while utilising torque vectoring to generate high sideslip. This is important as the human driver is responsible for the task of trajectory tracking and should not be disturbed by torque vectoring.

As illustrated in Figure 3(a) and (11), during corner entry, the predicted radius R_{pre} (which equals to R_{avg} in (9)) is simply calculated by averaging the preceding n timesteps, based on two assumptions: first, any change in trajectory radius within these timesteps is negligible; second, the driver could adjust the trajectory radius and achieve path tracking by steering, which won't be disturbed by the above averaging calculation. Similar design could also be found in [19] and [38], that steering is the only input responsible for yaw rate and path tracking.

For the phase of corner exit (after the apex point is found), in addition to R_{avg}, a second component R_{est} is particularly taken into account. It is determined by the time and radius at which the vehicle enters the corner (t_{enter}, R_{enter}) and reaches the apex point (t_{apex}, R_{apex}). As shown in Figure 3(a), (t_{enter}, R_{enter}) is determined when the current R_i drops below a

threshold (set here at 100 m), and (t_{apex}, R_{apex}) is determined by when $R_j < R_{j-1}$ and$R_j < R_{j+1}$. It is assumed that the relationship between trajectory radius R and time t could be described by a parabola (blue line in Figure 3a). As shown in Figure 3(b), through a rally track which will be utilised in the following sections of this paper, a good correlation could be observed between the parabola-based estimation R_{est} and the actual radius in the exit of the corners. Finally, with the above R_{avg} and R_{est}, a weighting function is implemented to calculate the predicted radius R_{pre} as illustrated in (11), in which w_1, w_2 are coefficients.

It is important to highlight the significance of the second part of prediction, R_{est}, especially in the scenario when the driver decides to activate the Drift Mode later than usual. For instance, while the vehicle is already exiting the corner, in this case the desired trajectory radius will increase significantly (i.e. the right half part of the parabola in Figure 3a). Consequently, relying solely on the first part of the prediction R_{avg}, which is based on an average of the previous timesteps, will result in a severe underestimation of the desired trajectory radius (red dots $R_{k-1}, \ldots, R_{k-n}$ in Figure 3a) and a disturbance to the driver's trajectory tracking task, leading the vehicle to the inner boundary of the track.

Concerns could be raised with respect to this 'Trajectory Radius Predictor' which partly relies on a 'parabola' assumption, simulation results on an asymmetrical track will be discussed in the following section of 'preliminary evaluations'.

$$R_{\text{avg}} = \frac{\sum_{i=1}^{n} R_{k-i}}{n} \tag{9}$$

$$R_{\text{est}} = \frac{R_{enter} - R_{apex}}{(t_{apex} - t_{enter})^2}[t - t_{apex}]^2 + R_{apex} \tag{10}$$

$$R_{pre} = w_1 R_{avg} + w_2 R_{est} \tag{11}$$

The Drift Mode (Mode 2)

Once the Drift Intention has been continuously detected for a certain amount of time, the vehicle switches to Drift Mode (Figures 1 and 2). In contrast to previous studies [16] where speed controllers are utilised to track the speed profile obtained from drift trajectory planning, this paper grants the driver complete control over the speed using throttle, as the focus is on drift assist control. However, unlike typical RWD vehicle which requires slip ratio regulation in order to achieve the desire sideslip [11], this study utilises the advantages of 4WD with independent wheel drive to assist the stabilisation of sideslip through torque vectoring, thereby reducing the requirement for advanced driving skills.

We assume the desired sideslip during the Drift Mode, denoted as β_d, could be determined according to the throttle input γ , as more throttle leads the vehicle drift deeper into the corner with higher sideslip. Therefore, we consider both the constant target sideslip like previous studies [16] and the contribution from the throttle input. The target sideslip β_d is written as (12), where for driver-in-loop test we set $\beta_{d0} = 10$ degrees as the default constant sideslip in Drift Mode, k_γ is the throttle gain of 15 degrees, γ is the throttle value from 0 to 1.

$$\beta_d = \beta_{d0} + k_\gamma \gamma \tag{12}$$

Next, we constrain the sideslip rate as (13) to allow the driver enough reaction time to counter steer when the sideslip is increased by torque vectoring, here τ is the time constant, and β is the current sideslip.

$$\dot{\beta}_d = \frac{1}{\tau}(\beta_d - \beta) \tag{13}$$

Then, taking the desired sideslip rate $\dot{\beta}_d$ from (13), and the predicted trajectory radius R_{pre} (11) into the equation of path angle rate and sideslip rate (8), the target yaw rate r_d for torque vectoring could be written as (14), which is a proven approach in autonomous drifting and path tracking control [15,23].

$$r_d = \dot{\varphi} - \dot{\beta}_d = \frac{v}{R_{pre}} - \frac{1}{\tau}(\beta_d - \beta) \tag{14}$$

Finally, given the target yaw rate r_d, we use the same method in Normal Mode to calculate the additional yaw moment M_z through (3) for subsequent torque vectoring controller, but it should be noted that the gains in (3) are calibrated separately between different drive modes.

The Sideslip Recovery Mode (Mode 3)

Once the Drift Intention is no longer detected (7), the vehicle switches to the Sideslip Recovery Mode (Mode 3) (Figures 1 and 2). This mode is designed to reduce the sideslip and transition to normal driving.

There has been limited research conducted on the exit mechanism of drifting, however, it is imperative after considering the behaviour of a human driver. It is crucial not to allow the rear axle regain lateral force too quickly, as this may cause an abrupt yaw moment (clockwise moment as shown in Figure 4 below) that pushes the vehicle towards the outer boundary of the track, which in turn requires the driver to perform timely steering to bring the vehicle back to the desired path. Therefore, just like a reverse process of the Drift Mode (Mode 2), in Sideslip Recovery Mode (Mode 3), we also limit the sideslip rate so the sideslip and the vector of combined force at the rear axle could be adjusted gradually, which results in smoother yaw motion of the vehicle, that allows the driver more response time in steering and achieve path tracking.

The difference compared to Drift Mode is that in Sideslip Recovery Mode we set the target sideslip β_d (12) as zero. The sideslip rate is constrained similarly as shown in (13), to provide the driver enough time to steer back from counter steering and quit drifting. Additionally, it is still important to take into account the predicted trajectory radius R_{pre} (11). Even though the sideslip is decreasing, the vehicle is still drifting and the path angle rate (8) has to be considered not only to assist the driver in path tracking, but also to calculate the target yaw rate, which could be written as (14).

After the target yaw rate is known, the desire yaw moment for torque vectoring control is calculated using the same approach as (3) but the gains are recalibrated.

The Counter-Steer Recovery Mode (Mode 4)

After the sideslip angle falls below a certain threshold value (the minimum sideslip of drift cornering from equilibrium analysis [49], also the maximum sideslip of normal cornering,

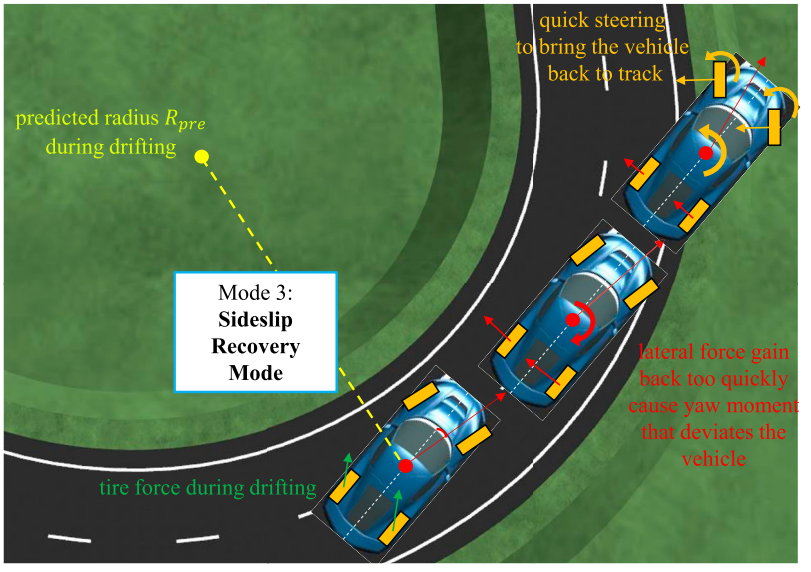


Figure 4. Why the rear axle should not gain back lateral force too quickly in Mode 3.

based on the 'bifurcation' dynamics [1,19,20]) while operating in the Sideslip Recovery Mode (Mode 3), occasionally we have observed one obstacle before the vehicle returns to Normal Mode (Mode 1). The presence of counter steering depicted as Mode 4 in Figure 2 will cause a significant challenge to the torque vectoring in Normal Mode (Mode 1) that calculates the additional yaw moment (3) according to the error between the actual yaw rate and the ideal yaw rate from steering (1). To be specific, if the system enters Normal Mode directly, counter steering will demand a clockwise yaw rate opposite to the current vehicle yaw motion. Hence it is necessary to introduce a Counter-Steer Recovery Mode (Mode 4) to eliminate counter steering (15) prior to entering Normal Mode (Mode 1).

$$r\delta < 0 \tag{15}$$

To design the Counter-Steer Recovery Mode (Mode 4), it is crucial to understand the reasons behind this abnormal 'residual counter steering' after successfully reducing sideslip in the Sideslip Recovery Mode (Mode 3). Two reasons have been concluded as shown in Figure 5: first, the driver steers too slowly back from counter steering; second, the driver intends to get closer to the outer edge of the track. For the first reason, even though the steering angle is directly controlled by the driver, it can still be influenced by sideslip control and torque vectoring, when a proper amount of negative yaw moment is applied to reduce the sideslip, and gently rotate the vehicle clockwise (on the left of Figure 5), the driver will reasonably end counter steering and steer to the left for trajectory tracking. For the second reason, since the driver desires to drive towards the outer boundary, the system should override the predicted radius, and a negative yaw moment as shown on the right of Figure 5 will help the driver to track the desired path and return from the abnormal counter steering.

In conclusion, for the concerned Counter-Steer Recovery Mode (Mode 4), the aim is to keep stabilising the sideslip regardless of the predicted trajectory radius. In addition, as the

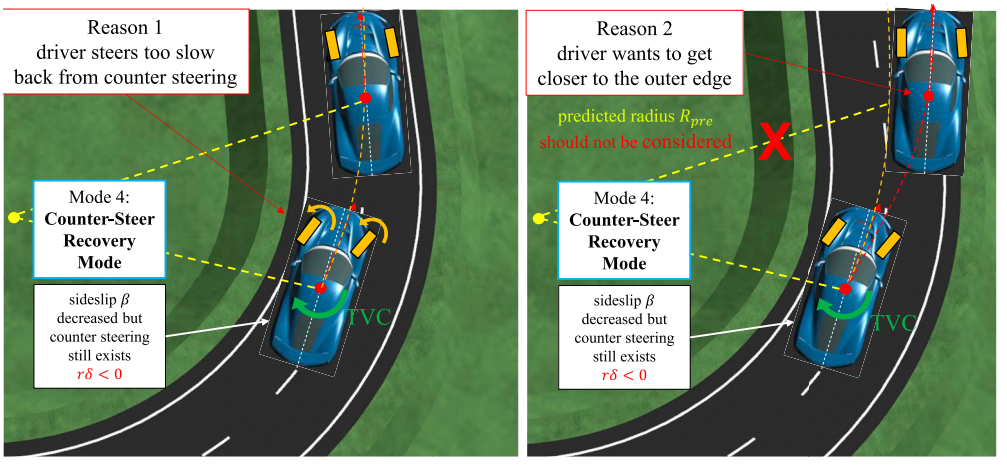


Figure 5. The reasons behind the abnormal counter steering after entering Mode 4.

sideslip is comparably small after exiting Sideslip Recovery Mode (Mode 3), it no longer disturbs the path angle rate (8) or the trajectory tracking task for the driver, therefore we consider the sideslip directly in the calculation of additional yaw moment from torque vectoring, as shown in (16), which will be used as the input for the torque vectoring controller in the following section:

$$M_z = k_p\beta + k_i \int \beta dt \tag{16}$$

The torque vectoring controller

After the desired yaw moment M_z ((3), (16)) from the abovementioned drive modes is obtained, the torque vectoring controller allocates the drive torque to four wheels. Together with the overall longitudinal drive force F_{xsum} decided by the throttle input from the driver, the drive force for each side of the wheels could be expressed as (17), in which w is the wheel track width.

$$F_{xl,xr} = 1/2F_{xsum} \mp M_z/w \tag{17}$$

To allocate $F_{xl,xr}$ between the front and rear wheels, in this paper a coefficient c_f is introduced to consider the load transfer between the front and rear axle. As indicated in (18), $F_{zf,zr}$ are the vertical loads of front and rear axle respectively, and c_{f0} is a constant offset coefficient. It is important to note that the value of c_{f0} varies for the aforementioned four drive modes. Particularly in Drift Mode, c_{f0} is larger than the other modes to deliver more torque to the rear wheels and ensure that the rear tires reach saturation before the front ones. This is necessary in drifting as the rear axle should be fully saturated [19].

$$c_f = \frac{F_{zf}}{F_{zf} + F_{zr}} - c_{f0} \tag{18}$$

$$\begin{aligned} F_{xfl,fr} &= c_f(1/2F_{xsum} \mp M_z/w) \\ F_{xrl,rr} &= (1 - c_f)(1/2F_{xsum} \mp M_z/w) \end{aligned} \tag{19}$$

Moreover, once the target longitudinal force $F_{xi}(i = fl, fr, rl, rr)$ has been defined, there is no slip ratio control involved for the wheels. Due to the over-actuated system features provided by 4WD with independent wheel torque control, also in line with the research of [44,45], we assume all the drive torque is delivered as tire force, as shown in (20).

$$T_{di} = F_{xi} r_w \tag{20}$$

Simulation and results

We introduce different scenarios to illustrate the operation of the proposed drift assist system. First, we present the result of a constant radius manoeuvre to highlight the importance of the proposed framework in drifting stabilisation against a more conventional torque vectoring system which simply produces an oversteering vehicle response. Second, we present the results from a sequence of corners to illustrate the system's transition from one mode to the other including crucially the distinction between counter steering and changing direction of corner. The efficacy of the proposed trajectory prediction method using the parabola approximation is tested in a scenario over a non-symmetric path. Finally, we present the results of implementing the drift assist system along the Pikes Peak track using both human driver-in-loop simulations and a commercial driver model available within the IPG Carmaker software.

Drift assist stabilisation versus a simplified yaw stability controller

Driver-in-loop results with drift assist on/off and an additional comparison with a simplified yaw stability controller are demonstrated in Figure 6. Specifically, the simplified yaw stability controller is based on the existing controllers in this paper from Mode 1 (yaw rate control according to steering input (3)) and Mode 4 (sideslip control (16)).

In contrast to the understeering vehicle without assist (steering angle increases during acceleration in Figure 6e), for the vehicle with the proposed drift assist control, once the 'Drift Intention' is recognised and enters Mode 2 (Figure 6a), the sideslip for drifting is generated and stabilised by torque vectoring (Figure 6d) meanwhile the driver performs counter steering smoothly in Figure 6(e), as the 'Trajectory Radius Predictor' helps to maintain the desired trajectory with limited lateral deviation (Figure 6f).

For the simplified yaw stability controller in comparison, high sideslip (Figure 6d) and drifting is indeed initiated without 'Drift Intention' recognition at around 150 m by subtly coordinating steering (Figure 6e) and throttle input (Figure 6b). However, the counter steering during drifting (i.e. 170 m in Figure 6e) results in an opposite desired yaw rate/moment to the corner and thus reduces the sideslip angle in Figure 6(d). Moreover, unlike our proposed framework (12–14), the desired sideslip angle during drifting is not explicitly considered in a simplified yaw stability controller. So, the drifting cannot be maintained continuously and requires more driving skills in throttle and steering (more oscillations in Figure 6b,e). Furthermore, due to the absence of the 'Trajectory Radius Predictor' which interprets the desired path angle rate, the simplified yaw stability controller is unable to help the driver in path tracking therefore more lateral deviation could be observed in Figure 6(f). Such finding agrees with the results in [15,23,32] that the path

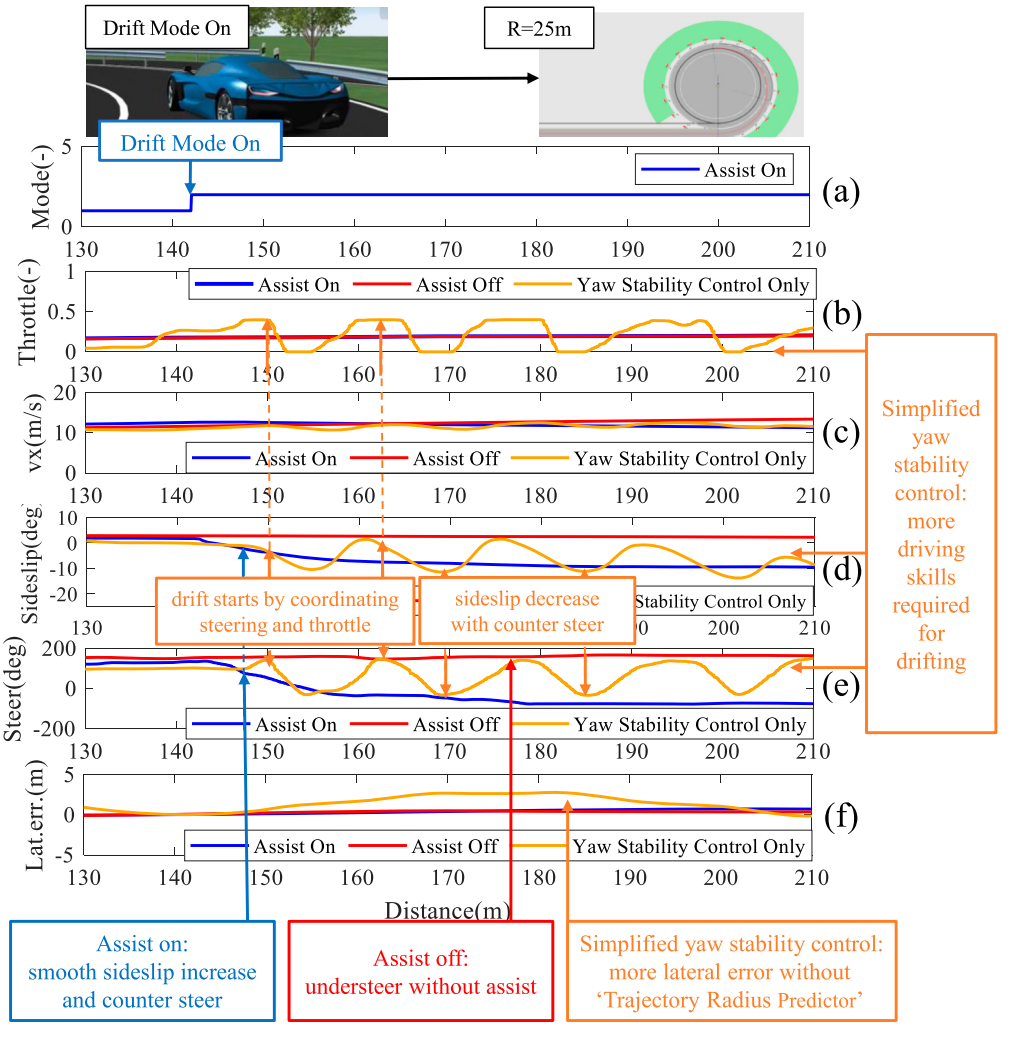


Figure 6. Simulation results of drift assist control on/off, and additional comparison with a simplified yaw stability controller on a fixed radius track.

angle rate should be considered rather than simply stabilising the yaw rate, otherwise the trajectory error will increase.

The above discussion indicates the following benefits of our proposed framework in comparison to a simplified yaw stability controller: (1) smooth drift entry (in terms of driver inputs) and maintenance due to 'Drift Intention' recognition; (2) the consideration of counter steering in the framework, and better sideslip stabilisation due to an explicit interpretation of the desired sideslip angle in our Drift Mode (12–13), therefore requires less driving skill for drift maintenance; (3) better path tracking performance, due to the 'Trajectory Radius Predictor' which considers the path angle rate (14).

Evaluations in a sequence of corners

The second scenario is an 'S-Turn' track built in CarMaker and implemented with a human driver-in-loop (video at: https://www.youtube.com/watch?v=1p8AyHKGkB8). As shown

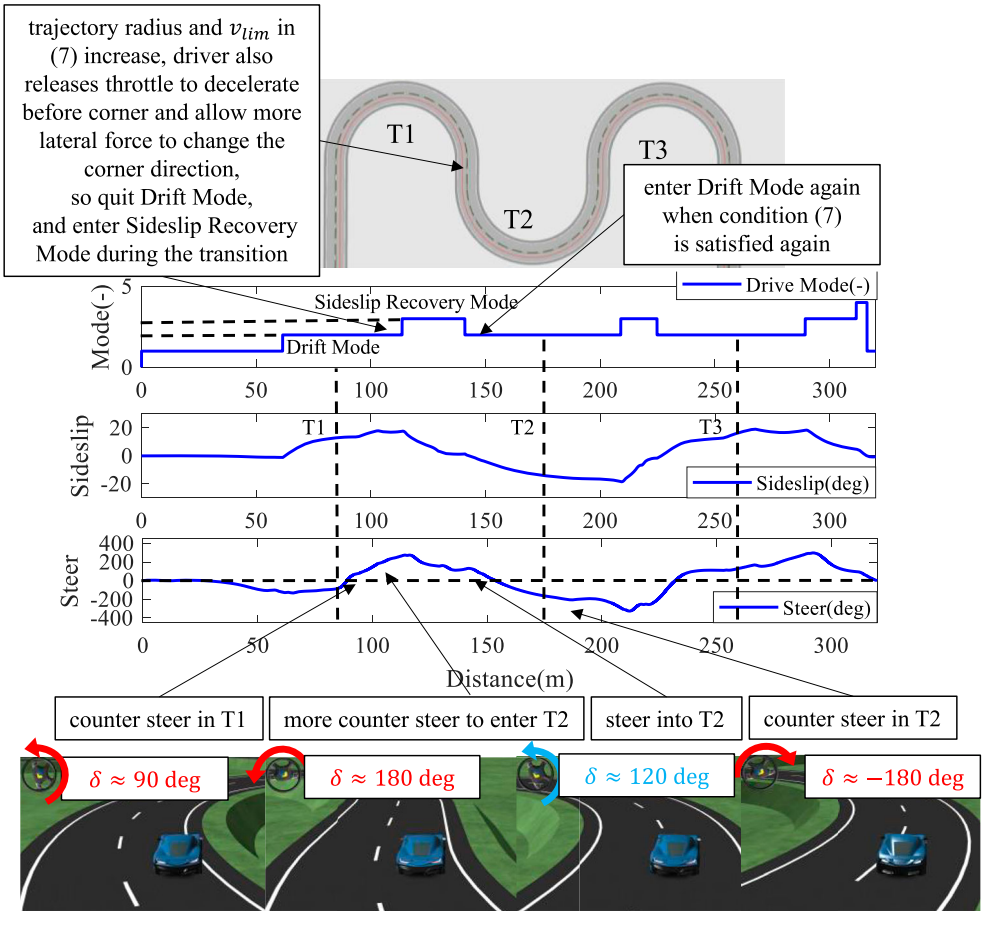


Figure 7. Simulation results with drift assist control on S-Turn track (video at: https://www.youtube.com/watch?v=1p8AyHKGkB8).

in Figure 7, when the driver keeps counter steering in the end of T1 to enter T2, the trajectory radius and v_{lim} in (7) increase, meanwhile the driver releases the throttle shortly to decelerate before corner, also to allow the rear axle more lateral force to change the corner direction, which will lead the system to quit Drift Mode and enter Sideslip Recovery Mode for a very short period according to the 'Drift Intention' condition in (7). Until the driver enters the next corner, the above condition will be satisfied and the Drift Mode will be activated again.

Evaluations in asymmetrical-shaped corners

In this scenario, we illustrate the ability of the control framework to accommodate asymmetric paths despite the simplifying 'parabola' assumption in the 'Trajectory Radius Predictors'. In Figure 8, a track with varying radius is considered in human driver in the loop simulation (video at https://www.youtube.com/watch?v=7preJkxoRe8). The driver

successfully drifts in the corners with reducing/increasing radius respectively. The reason is as follows: in contrast to 'hairpin' corners, in long corners where the radius doesn't change abruptly, an average of the history radius R_{avg} as shown in the bottom of Figure 8 is enough for prediction, therefore the weight w_1 of R_{avg} is increased accordingly. We should highlight here that this work focuses on the design of the framework, and an improved trajectory radius prediction is being developed and will be elaborated in our future work.

The Pikes Peak track

To evaluate our proposed framework for drift assist control, part of the Pikes Peak track is utilised for simulation in IPG CarMaker, the track layout is shown in Figure 9. There are a total of eight corners on the track where the vehicle performs drifting.

The CarMaker driver model results on Pikes Peak and analysis

In contrast to the previous studies relying on specific drifting path planning [16,32,47] or drift path-following controllers [15,46] to produce desired vehicle motions, we first use a standard path-following driver model from CarMaker to emulate the behaviours of a human driver and evaluate our drift assist control framework (video at https://www.youtube.com/watch?v=oW0LCQXVhJQ).

Specifically, we consider two particular cornering methods to validate the robustness of our control, namely Early Braking (EB) and Trail Braking (TB) respectively, as depicted in Figure 10. For EB, the driver tends to brake earlier on the straight line prior to entering the corner (i.e. for T2–T4 in Figure 10b), and apply the throttle to accelerate more aggressively throughout the corner (Figure 10c). For TB, the driver brakes later and deeper while entering the corner, then gradually applies throttle in the exit of the corner.

As shown in Figure 10(d), take T2 as an example, the system can effectively detect the Drift Intention to perform drifting in the concerned corner. The system seamlessly transits through Modes 1–4. And the variation in the cornering styles (EB & TB) doesn't significantly disrupt the functionality of the drift assist control framework.

The sideslip and steering results

As for the sideslip which is increased during the drifting in T2, as depicted in Figure 10(e), in EB since the driver steps on the throttle more aggressively through the corner, and the Drift Modes lasts longer as in Figure 10(d), therefore the maximum sideslip of EB (blue line in Figure 10e) is slightly higher than TB (red line) due to the calculation of the desired sideslip based on the throttle input.

With respect to the steering behaviour, as shown in Figure 10(f), due to the relationship between equilibrium sideslip and counter steering angle during drifting [19], higher sideslip during EB demands more counter steering, which could be observed in Figure 10(f).

In general, due to the limited sideslip rate, enough reaction time is guaranteed for the driver to perform steering during sideslip variation. This not only aids in effectively maintaining the trajectory radius with lateral deviation less than 1 m in all eight corners (Figure 10g), but also partially indicates the intuitive nature of the proposed control framework, as well as its robustness against different cornering styles.

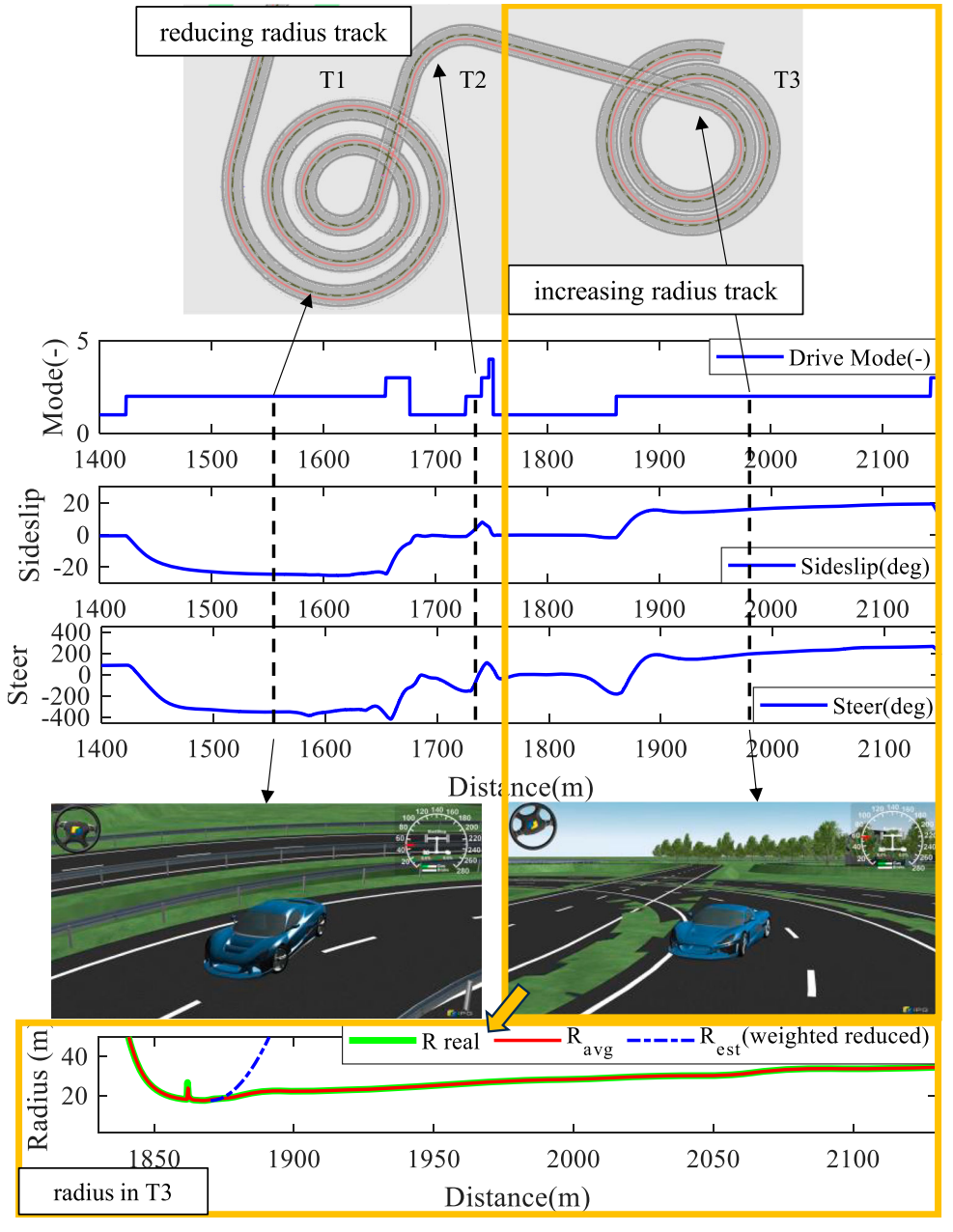


Figure 8. Simulation results with drift assist control on varying radius track (video at: https://www.youtube.com/watch?v=7preJkxoRe8).

The wheel drive torque results

In terms of wheel torque, the drive torque for four wheels is demonstrated in Figure 11(b). Taking the seventh corner (T7, left turn) with TB cornering as a case study, in Drift Mode there is a continuous positive yaw moment (Figure 11f) that rotates the vehicle counter-clockwise to increase the sideslip angle (Figure 11d). Once Sideslip Recovery Mode is

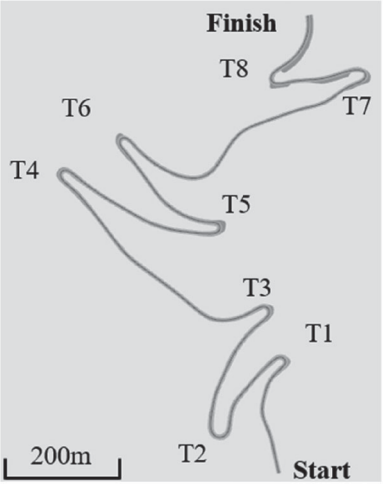


Figure 9. The track layout of Pikes Peak rally track.

activated, the yaw moment turns negative very shortly to reduce the sideslip, then returns to positive values to regulate the sideslip rate and path angle rate as in (14). Then in Counter-Steer Recovery Mode, the aim is solely to reduce the sideslip angle without imposing rate limits, so the yaw moment turns negative until there is no more counter steering (Figure 11e).

In addition, the continuous positive yaw moment produced by TVC during drifting indicates that TVC between left/right wheels could further expand the current known 4WD equilibrium region from [40], that steady-state drifting could be stabilised by TVC without using a particular set of equilibrium results as reference, but at the cost of requiring a continuous yaw moment generated by TVC, which agrees with previous studies [44–46]. The above phenomena illustrates that our proposed method (that allows the driver to select a sideslip angle during drift stabilisation based on throttle input [49]) is not limited by a set of known steady-state conditions.

The driving simulator and driver-in-loop test results on Pikes Peak

Aside from employing the standard driver model in IPG CarMaker, we further utilise the driving simulator in Cranfield University (Figure 12) and incorporate a human driver with no professional racing or drifting background to verify our drift assist control framework (video at: https://www.youtube.com/watch?v=02aSdlMkZlg).

In general, the system successfully detects the Drift Intention and switches to Drift Mode in the eight concerned corners. As shown in Figure 13, when the Drift Mode is triggered and the sideslip is increased by torque vectoring, the driver could intuitively counter steer and then return to neutral steering position when the sideslip is reduced in Mode 3 and 4. Moreover, due to the constrained sideslip rate, the driver has sufficient time to respond and adjust the steering while the sideslip changes, therefore successfully stays on the intended track.

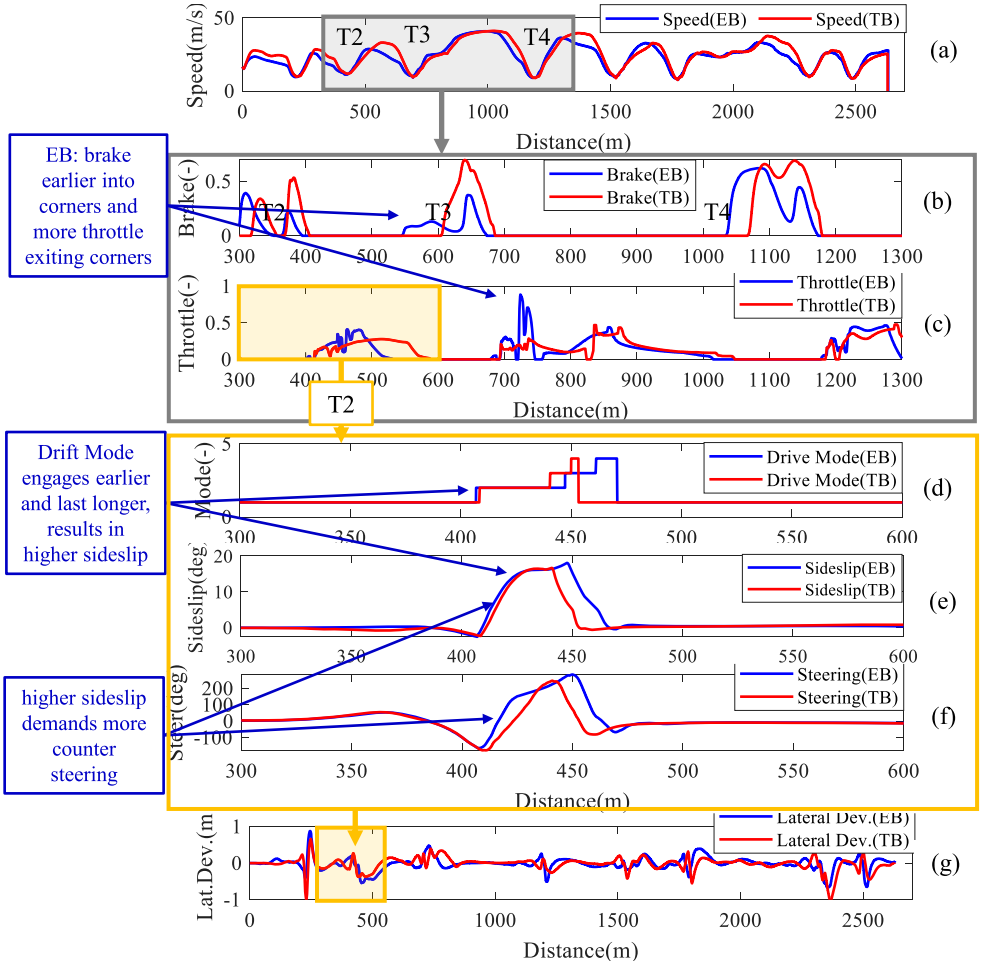


Figure 10. The CarMaker driver model with different cornering methods on Pikes Peak.

Interestingly, in contrast to the CarMaker driver model results (Figure 11), in Figure 13 for corners like T8 the system doesn't go into Counter-Steer Recovery Mode (Mode 4), and in T2 the system directly returns to Normal Mode (Mode 1) from Drift Mode (Mode 2). For T8, the detailed driver inputs and vehicle behaviours are shown in Figure 14. It could be seen that the sideslip is already reduced significantly in Drift Mode due to the decreased throttle input, therefore the Sideslip Recovery Mode (Mode 3) doesn't last long till the sideslip returns to the normal region. Also, after performs counter steering during drifting, the driver steers towards neutral position timely and the counter steering angle is low, therefore it is unnecessary for the system to go through the Counter-Steer Recovery Mode (Mode 4) before return to Normal Mode.

As for T2, the driver inputs and vehicle behaviour are demonstrated in Figure 15. Similar to the behaviour in T8 discussed above, the sideslip is already gradually reduced to a relatively low level in the end of Drift Mode due to the absence of throttle input, also the steering is back to neutral position together with the sideslip, therefore it is unnecessary to transition through Mode 3 or 4 anymore so the system directly returns to Normal Mode.

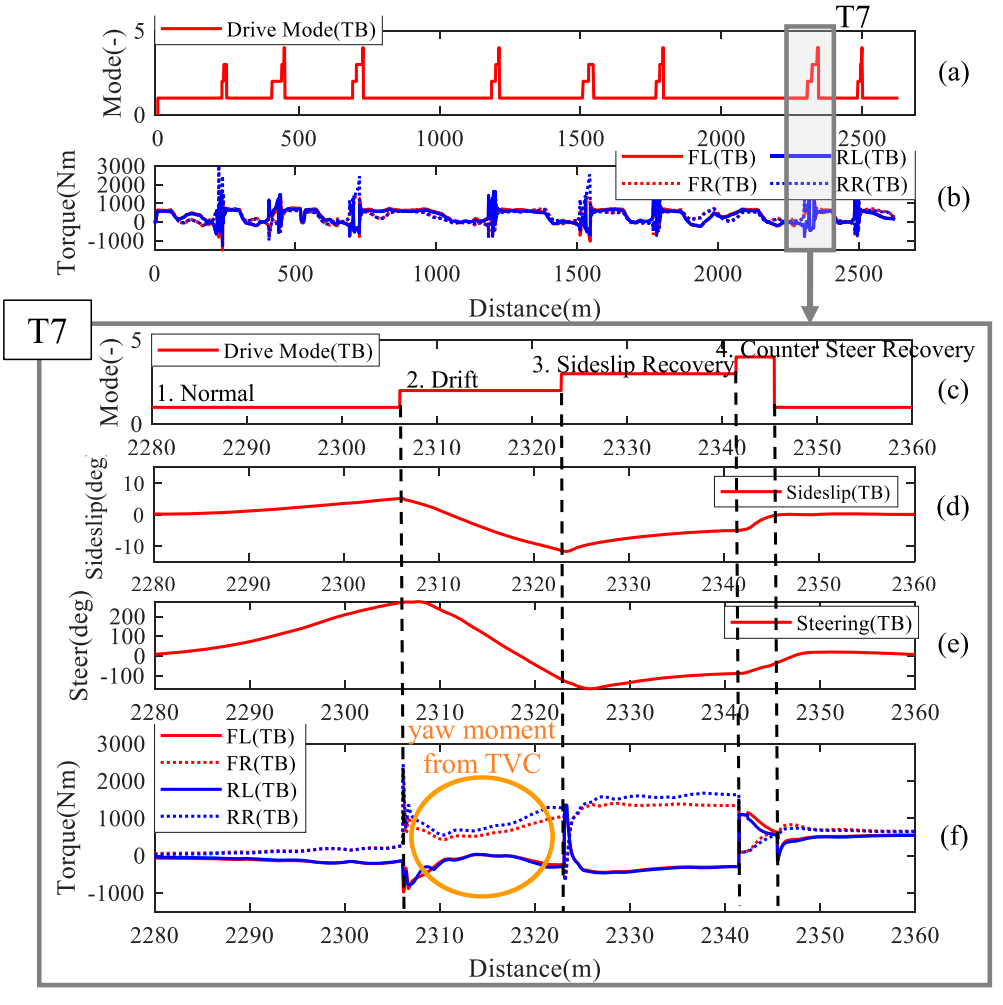


Figure 11. The wheel torque during the seventh corner (T7) on Pikes Peak with TB cornering (video at: https://www.youtube.com/watch?v=oW0LCQXVhJQ).

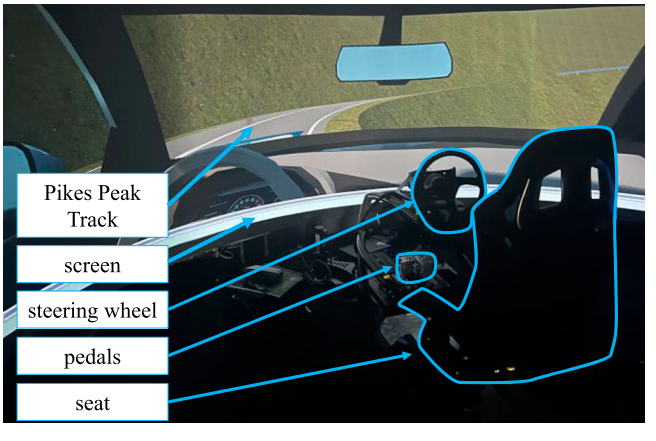


Figure 12. The driving simulator in Cranfield University.

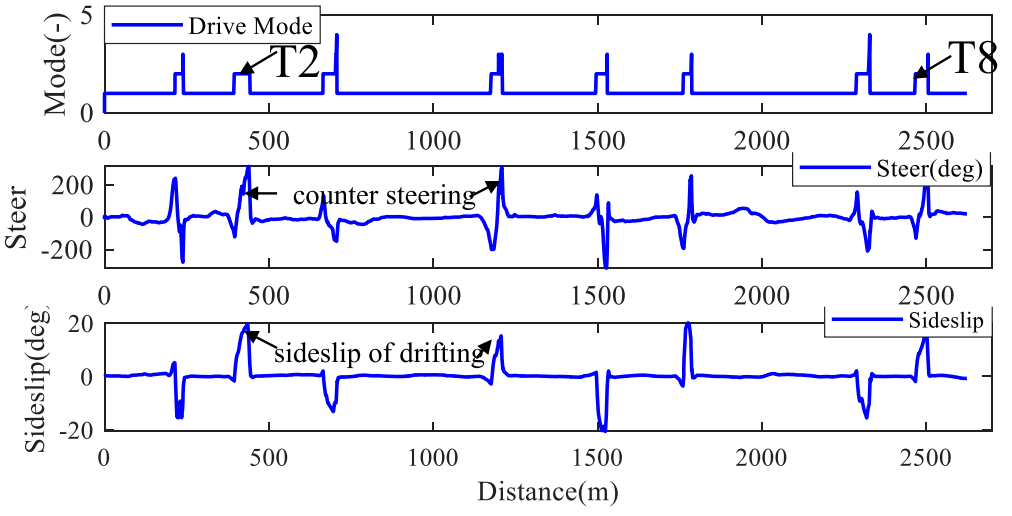


Figure 13. The drive mode transition and sideslip on Pikes Peak with a human driver (video at: https://www.youtube.com/watch?v=02aSdlMkZlg).

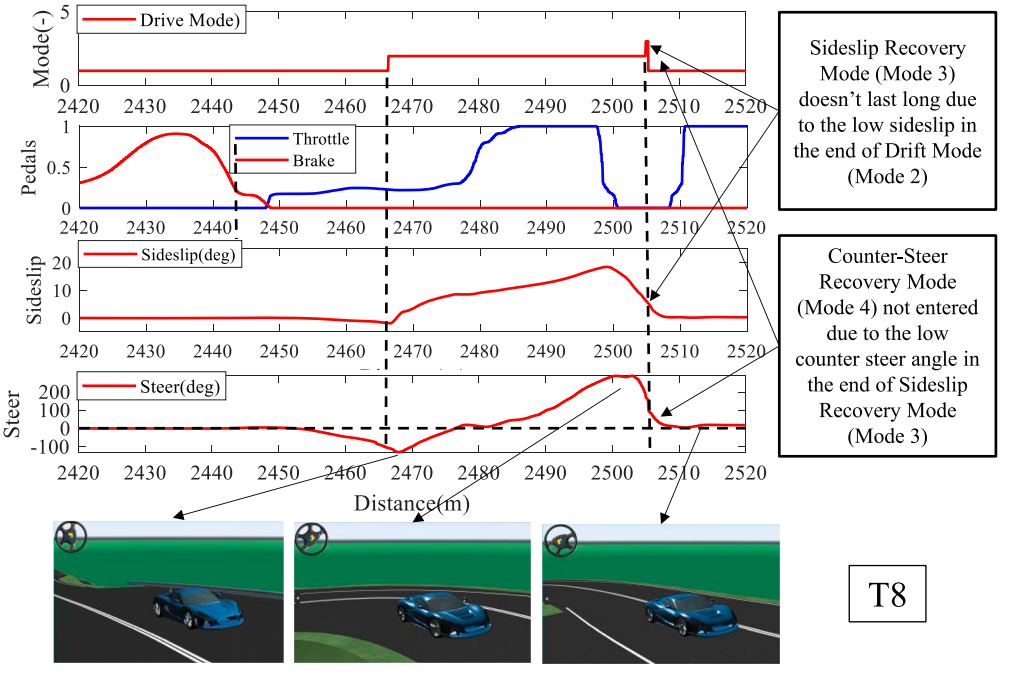


Figure 14. The vehicle behaviour at T8 of Pikes Peak with human driver.

Conclusion

In this paper, we present a novel state machine-based 4WD drift assist controller with four drive modes, to allow the driver transition into and out of drifting in corners intuitively.

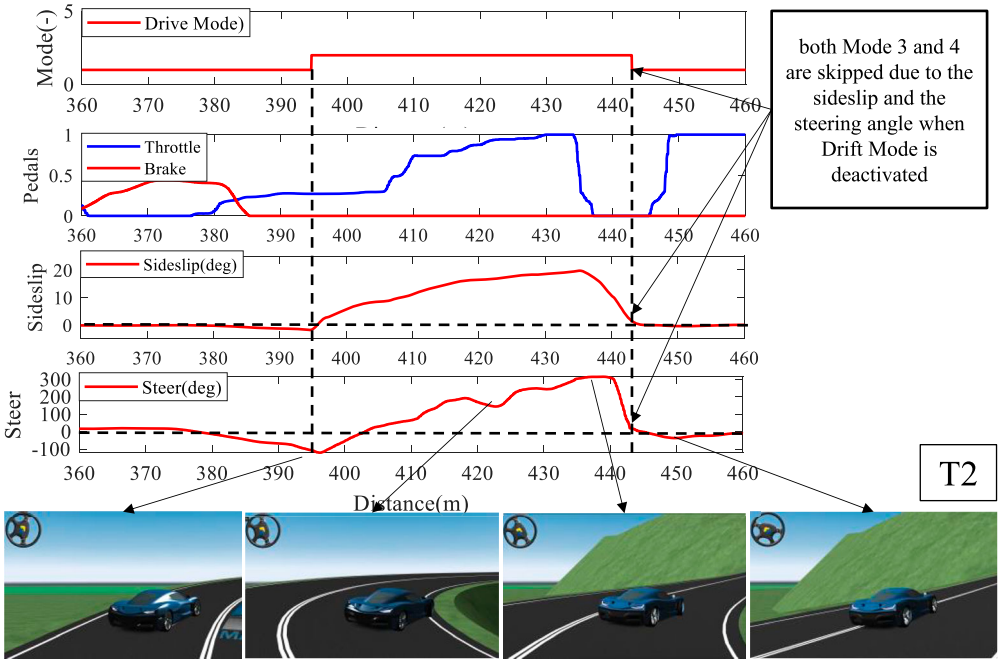


Figure 15. The vehicle behaviour at T2 of Pikes Peak with human driver.

To interpret the driver's intention to start/end drifting, no additional control inputs such as buttons or switches are used. Instead, we rely on the pedals, steering and other basic motion signals to identify the driver's 'Drift Intention'.

Furthermore, during drifting, in contrast to previous studies relying on prior knowledge of track radius, we introduce a 'Trajectory Radius Predictor' to estimate the corner curvature, in order to assist the driver stay on course and provide reference yaw rate to the subsequent torque vectoring controller.

Moreover, for drifting sideslip stabilisation, thanks to the over-actuated feature of 4WD electric vehicle with independent wheel torque control, no precalculated drift equilibrium is involved as control target. Besides, we restrict the sideslip rate during drifting to allow the driver enough reaction time to adjust the steering when the sideslip changes.

To validate our control framework, the Pikes Peak rally track in IPG CarMaker is utilised, and we consider different driving behaviours from both the CarMaker driver model and a human driver using the driving simulator of Cranfield University. The simulation results have proven the effectiveness and robustness of the proposed framework, that the driver is able to drift the vehicle in the desired corners.

Future work

In this paper, our scope is more about proposing the general framework of our drift assist control system, and there are several limitations we are going to explore and improve in our future work. First, for road friction, in this paper we treat it as a known parameter, which in reality needs estimation. An estimator will be proposed to further evaluate the

robustness of the system and the performance in practical implementation. Second, for the driver's 'Drift Intention', a model which could consider more detailed driver behaviour features (i.e. steering behaviour) is being developed to activate/deactivate the Drift Mode more intuitively. Third, for the 'Trajectory Radius Predictor' in this paper, the 'parabola' assumption is mainly limited to hairpin shaped corners. Though drifting could be successful achieved in asymmetrical-shaped corner as discussed in 'Preliminary evaluations' section, we are currently working on an improved trajectory prediction model, which is not only based on vehicle dynamics model, but also able to interpret the desired trajectory from driver's pattern level and path planning level. Moreover, as for the torque vectoring controller, in this paper we are utilising the advantage of 4WD with independent wheel drive and therefore ignoring the constraints in tire force allocation and utilisation, which should be explored and discussed with advanced control approach to achieve better drifting performance and robustness in real-world application.

Acknowledgments

The financial and intellectual contributions of Rimac Technology are acknowledged for their role in supporting this research.

Disclosure statement

No potential conflict of interest was reported by the author(s).

References

[1] Ono E, Hosoe S, Hoang DT, et al. Bifurcation in vehicle dynamics and robust front wheel steering control. IEEE Trans Control Syst Technol. 1998;6(3):412–420. doi:10.1109/87.668041
[2] Abdulrahim M. On the dynamics of automobile drifting; 2006. [Online]. doi:10.4271/2006-01-1019
[3] Velenis E. FWD vehicle drifting control: the handbrake-cornering technique. In: 2011 50th IEEE Conference on Decision and Control and European Control Conference; 2011 Dec 12–15; 2011. p. 3258–3263. doi:10.1109/CDC.2011.6161195
[4] Tavernini D, Velenis E, Lot R, et al. The optimality of the handbrake cornering technique. J Dyn Syst Meas Control. 2014;136:4. doi:10.1115/1.4026836
[5] Edelmann J, Plöchl M, Lugner P, et al. Investigations on the powerslide of automobiles. In: Proceedings of AVEC'08; 2008.
[6] Velenis E, Tsiotras P, Lu J. Modeling aggressive maneuvers on loose surfaces: the cases of Trail-Braking and Pendulum-Turn. In: 2007 European Control Conference (ECC); 2007 Jul 2–5; 2007. pp. 1233–1240. doi:10.23919/ECC.2007.7068670
[7] Velenis E, Tsiotras P, Lu J. Aggressive maneuvers on loose surfaces: data analysis and input parametrization. In: 2007 Mediterranean Conference on Control & Automation; 2007 Jun 27–29; 2007. pp. 1–6. doi:10.1109/MED.2007.4433885
[8] Edelmann J, Plöchl M. Handling characteristics and stability of the steady-state powerslide motion of an automobile. Regul Chaotic Dyn. 2009;14(6):682–692. doi:10.1134/S1560354709060069
[9] Liaw DC, Chiang HH, Lee TT. Elucidating vehicle lateral dynamics using a bifurcation analysis. IEEE Trans Intell Trans Syst. 2007;8(2):195–207. doi:10.1109/TITS.2006.888598
[10] Velenis E, Frazzoli E, Tsiotras P. Steady-state cornering equilibria and stabilisation for a vehicle during extreme operating conditions. Int J Veh Auton Syst. 2010;8:217–241.
[11] Velenis E, Katzourakis D, Frazzoli E, et al. Steady-state drifting stabilization of RWD vehicles. Control Eng Pract. 2011;19(11):1363–1376. doi:10.1016/j.conengprac.2011.07.010

[12] Baur M, Bascetta L. An experimentally validated LQR approach to autonomous drifting stabilization. In: 2019 18th European Control Conference (ECC); 2019 Jun 25–28; 2019. pp. 732–737. doi:10.23919/ECC.2019.8795883
[13] Goh JY, Gerdes JC. Simultaneous stabilization and tracking of basic automobile drifting trajectories. In: 2016 IEEE Intelligent Vehicles Symposium (IV); 2016 Jun 19–22; 2016. pp. 597–602. doi:10.1109/IVS.2016.7535448
[14] Park M, Kang Y. Experimental verification of a drift controller for autonomous vehicle tracking: a circular trajectory using LQR method. Int J Control Autom Syst. 2021;19(1):404–416. doi:10.1007/s12555-019-0757-2
[15] Goh JY, Goel T, Christian Gerdes J. Toward automated vehicle control beyond the stability limits: drifting along a general path. J Dyn Syst Meas Contr. 2020;142:2, doi:10.1115/1.4045320
[16] Acosta Reche M, Kanarachos S, Fitzpatrick M. A hybrid hierarchical rally driver model for autonomous vehicle agile maneuvering on loose surfaces. Paper presented at: the International Conference on Informatics in Control, Automation and Robotics; 2017.
[17] Kritayakirana K, Gerdes J. Autonomous vehicle control at the limits of handling. Int J Veh Auto Syst. 2012;10:271–296. doi:10.1504/IJVAS.2012.051270
[18] Baars M, Hellendoorn H, Alirezaei M. Control of a scaled vehicle in and beyond stable limit handling. IEEE Trans Vehicular Tech. 2021;70(7):6427–6437. doi:10.1109/TVT.2021.3085503
[19] Voser C, Hindiyeh RY, Gerdes JC. Analysis and control of high sideslip manoeuvres. Veh Syst Dyn. 2010;48(sup1):317–336. doi:10.1080/00423111003746140
[20] Hindiyeh RY, Gerdes JC. Equilibrium analysis of drifting vehicles for control sesign; 2009. [Online]. doi:10.1115/DSCC2009-2626
[21] Velenis E, Frazzoli E, Tsiotras P. On steady-state cornering equilibria for wheeled vehicles with drift. In: Proceedings of the 48h IEEE Conference on Decision and Control (CDC) held jointly with 2009 28th Chinese Control Conference; 2009 Dec 15–18; 2009. pp. 3545–3550. doi:10.1109/CDC.2009.5399782
[22] Zubov I, Afanasyev I, Gabdullin A, et al. Autonomous Drifting Control in 3D Car Racing Simulator. In: 2018 International Conference on Intelligent Systems (IS); 2018 Sept 25–27; 2018. pp. 235–241. doi:10.1109/IS.2018.8710588
[23] Hindiyeh RY, Gerdes JC. A controller framework for autonomous drifting: design, stability, and experimental validation. J Dyn Syst Meas Contr. 2014;136:5. doi:10.1115/1.4027471
[24] Gonzales J, Zhang F, Li K, et al. Autonomous drifting with onboard sensors. Paper presented at: The 13th International Symposium on Advanced Vehicle Control (AVEC' 16); 2016 Sept 13–16; Munich, Germany.
[25] Gray A, Gao Y, Lin T, et al. Predictive control for agile semi-autonomous ground vehicles using motion primitives. In: 2012 American Control Conference (ACC); 2012 Jun 27–29; 2012. pp. 4239–4244. doi:10.1109/ACC.2012.6315303
[26] Hu C, Zhou X, Duo R, et al. Combined fast control of drifting state and trajectory tracking for autonomous vehicles based on MPC controller. In: 2022 International Conference on Robotics and Automation (ICRA); 2022 May 23–27; 2022. pp. 1373–1379. doi:10.1109/ICRA46639.2022.9812185
[27] Dong H, Yu H, Xi J. Real-time model predictive control for simultaneous drift and trajectory tracking of autonomous vehicles. In: 2022 6th CAA International Conference on Vehicular Control and Intelligence (CVCI); 2022 Oct 28–30; 2022. pp. 1–6. doi:10.1109/CVCI56766.2022.9964790
[28] Xu D, Han Y, Ge C, et al. A model predictive control method for vehicle drifting motions with measurable errors. World Electr Veh J. 2022;13(3):54. doi:10.3390/wevj13030054
[29] Guo H, Tan Z, Liu J, et al. MPC-based steady-state drift control under extreme condition. In: 2021 33rd Chinese Control and Decision Conference (CCDC); 2021 May 22–24; 2021. pp. 4708–4712. doi:10.1109/CCDC52312.2021.9602572
[30] Chen G, Zhao X, Gao Z, et al. Dynamic drifting control for general path tracking of autonomous vehicles. IEEE Trans Intell Veh. 2023;8(3):2527–2537. doi:10.1109/TIV.2023.3235007

[31] Kim M, Lee T, Kang Y. Experimental verification of the power slide driving technique for control strategy of autonomous race cars. Int J Prec Eng Manuf. 2020;21(3):377–386. doi:10.1007/s12541-019-00263-1
[32] Joa E, Cha H, Hyun Y, et al. A new control approach for automated drifting in consideration of the driving characteristics of an expert human driver. Control Eng Pract. 2020;96:104293, doi:10.1016/j.conengprac.2019.104293
[33] Vignati M, Sabbioni E, Cheli F. A torque vectoring control for enhancing vehicle performance in drifting. Electronics. 2018;7(12):394. doi:10.3390/electronics7120394
[34] Pereiras VF. Drift control with driver in the loop. MSc, School of Aerospace, Transport and Manufacturing, Cranfield University; 2022.
[35] GmbH BM. The M drift analyser for BMW M3 and M4. https://www.bmw-m.com/en/topics/magazine-article-pool/bmw-m3-m4-m-drift-analyser.html.
[36] Miller B. McLaren variable drift control: does it work? https://www.carmagazine.co.uk/car-news/tech/mclaren-variable-drift-control-how-does-it-work/.
[37] Duff M. Thank you for smoking: ford explains the focus RS's "Drift Mode". https://www.caranddriver.com/news/a15357160/thank-you-for-smoking-ford-explains-the-focus-rss-drift-mode/.
[38] Werling M, Reinisch P, Groell L. Robust power-slide control for a production vehicle. Int J Veh Auto Syst. 2015;13:27. doi:10.1504/IJVAS.2015.070727
[39] Joa E, Yi K, Hyun Y. Autonomous drift control using vehicle lateral dynamics with self-rotation and revolution; 2018.
[40] Milani S, Marzbani H, Jazar RN. Vehicle drifting dynamics: discovery of new equilibria. Veh Syst Dyn. 2022;60(6):1933–1958. doi:10.1080/00423114.2021.1887499
[41] Hou X, Zhang J, Ji Y, et al. Autonomous drift controller for distributed drive electric vehicle with input coupling and uncertain disturbance. ISA Trans. 2022;120:1–17. doi:10.1016/j.isatra.2021.03.009
[42] Tian X, Yang S, Yang Y, et al. A multi-layer drifting controller for all-wheel drive vehicles beyond driving limits IEEE/ASME Trans Mechatron 2024;29(2):1229–1239. doi:10.1109/TMECH.2023.3298660
[43] Yang B, Lu Y, Yang X, et al. A hierarchical control framework for drift maneuvering of autonomous vehicles. In: 2022 International Conference on Robotics and Automation (ICRA); 2022 May 23–27; 2022. pp. 1387–1393. doi:10.1109/ICRA46639.2022.9812110
[44] Nakano H, Kinugawa J, Kosuge K. Control of a four-wheel independently driven electric vehicle with a large sideslip angle. In: 2014 IEEE International Conference on Robotics and Biomimetics (ROBIO 2014); 2014Dec 5–10; 2014. 265–270. doi:10.1109/ROBIO.2014.7090341
[45] Nakano H, Okayama K, Kinugawa J, et al. Control of an electric vehicle with a large sideslip angle using driving forces of four independently-driven wheels and steer angle of front wheels. In: 2014 IEEE/ASME International Conference on Advanced Intelligent Mechatronics; 2014 Jul 8–11; 2014. pp. 1073–1078. doi:10.1109/AIM.2014.6878223
[46] Nakano H, Kinugawa J, Kosuge K. Trajectory tracking control of a vehicle with a large sideslip angle. In: 2015 IEEE International Conference on Advanced Intelligent Mechatronics (AIM); 2015. pp. 971–976. doi:10.1109/AIM.2015.7222665
[47] Acosta M, Kanarachos S, Blundell M. Vehicle agile maneuvering: from rally drivers to a finite state machine approach. In: 2016 IEEE Symposium Series on Computational Intelligence (SSCI); 2016 Dec 6–9; 2016. pp. 1–8. doi:10.1109/SSCI.2016.7850095
[48] Sun Y, Velenis E, Krishnakumar A. Steering noise cancelling for drift assist control. In: G. Mastinu, F. Braghin, F. Cheli, M. Corno, and S. M. Savaresi, editors. 16th International Symposium on Advanced Vehicle Control, Cham: Springer Nature Switzerland; 2004. pp. 618–624.
[49] Sun Y, Velenis E, Krishnakumar A. Evaluation of an intuitive 4WD drift assist control concept in a driving simulator. Veh Syst Dyn. 2025;1–22. doi:10.1080/00423114.2025.2487186



https://dspace.org/

A 4WD drift assist control framework on general rally track

Sun, Yiwen; Velenis, Efstathios; Krishnakumar, Ajinkya

2025-12-31
Taylor & Francis
https://doi.org/10.1080/00423114.2025.2556928
Sun Y, Velenis E, Krishnakumar A. (2025) A 4WD drift assist control framework on general rally track. Vehicle System Dynamics, Available online 15 September 2025

Downloaded from a DSpace repository. https://dspace.org/